

Optimal Household Appliances Scheduling under Day-Ahead Pricing and Load-Shaping Demand Response Strategies

Nikolaos G. Paterakis, *Student Member, IEEE*, Ozan Erdinc, *Member, IEEE*, Anastasios G. Bakirtzis, *Fellow, IEEE*, and João P. S. Catalão, *Senior Member, IEEE*

Abstract—In this paper, a detailed Home Energy Management System structure is developed in order to determine the optimal day-ahead appliance scheduling of a smart-household under hourly pricing and peak power limiting (hard and soft power limitation) based demand response (DR) strategies. All types of controllable assets have been explicitly modeled, including thermostatically controllable (air conditioners and water heaters) and non-thermostatically controllable (washing machines and dishwashers) appliances, together with electric vehicles (EV). Furthermore, an energy storage system (ESS) and distributed generation at the end-user premises are taken into account. Bi-directional energy flow is also considered through advanced options for EV and ESS operation. Finally, a realistic test-case is presented with a sufficiently reduced time granularity, being thoroughly discussed in order to investigate the effectiveness of the model. Stringent simulation results are provided using data gathered from real appliances and real measurements.

Index Terms—demand response, distributed generation, electric vehicles, energy storage system, home energy management, smart household.

I. NOMENCLATURE

The main nomenclature used throughout the paper is stated below.

A. Sets

m set of shifting appliances.
 p set of operating phases of appliances.
 t set of time periods.

B. Parameters

a ratio of increase over maximum daily price for pricing excessive power drawn from the grid.
 A_i element area [m^2].
 c_a thermal capacity of air [$\text{kJ/kg}\cdot^\circ\text{C}$].
 C EWH thermal capacitance [$\text{kWh}/^\circ\text{C}$].

CE^{ESS} charging efficiency of ESS.
 CE^{EV} charging efficiency of EV.
 COP coefficient of performance.
 DE^{ESS} discharging efficiency of ESS.
 DE^{EV} discharging efficiency of EV.
 L_t inflexible load [kW].
 l_i element thickness [m].
 L_1 house length [m].
 L_2 house width [m].
 L_3 house height [m].
 M_a mass of air [kg].
 M electric water heater (EWH) tank size [gallons].
 m_t hot water usage [gallons].
 N_m number of times an appliance has to be operated during a day.
 PL_1 upper limit for the power drawn from the grid [kW].
 PL_2 upper limit for the power sold back to the grid [kW].
 PL_1^t time varying upper limit for the power drawn from the grid [kW].
 P_{AC} AC rated power [kW].
 $P_t^{PV,PRO}$ available PV power [kW].
 $P_{m,p}^{ph}$ rated power of an operating phase of a cycle of a non-thermostatically controllable appliance [kW].
 Q EWH capacity [kW].
 R EWH thermal resistance [$^\circ\text{C}/\text{kW}$].
 R^{eq} equivalent thermal resistance [$\text{h}\cdot^\circ\text{C}/\text{J}$].
 $R^{ESS,ch}$ ESS charging rate [kW].
 $R^{ESS,dis}$ ESS discharging rate [kW].
 $R^{EV,ch}$ EV charging rate [kW].
 $R^{EV,dis}$ EV discharging rate [kW].
 $SOE^{ESS,ini}$ initial SOE of ESS [kWh].
 $SOE^{ESS,max}$ maximum SOE of EV [kWh].
 $SOE^{ESS,min}$ minimum SOE of EV [kWh].
 $SOE^{EV,ini}$ initial SOE of EV [kWh].
 $SOE^{EV,max}$ maximum SOE of EV [kWh].
 $SOE^{EV,min}$ minimum SOE of EV [kWh].
 SP_t AC temperature set-point [$^\circ\text{C}$].
 T^a EV arrival time.
 T_t^a outdoor air temperature [$^\circ\text{C}$].
 T^d EV departure time.
 $T_{m,p}^{dur}$ duration of a cycle of an operating phase of a non-thermostatically controllable appliance [periods].
 $T_t^{c,w}$ inlet water temperature [$^\circ\text{C}$].
 $T^{h,w,min}$ minimum hot water temperature [$^\circ\text{C}$].

This work was supported by FEDER funds (European Union) through COMPETE and by Portuguese funds through FCT, under Projects FCOMP-01-0124-FEDER-020282 (Ref. PTDC/EEA-EEL/118519/2010) and UID/CEC/50021/2013. Also, the research leading to these results has received funding from the EU Seventh Framework Programme FP7/2007-2013 under grant agreement no. 309048 (project SiNGULAR).

N. G. Paterakis and J. P. S. Catalão are with the Univ. Beira Interior, Covilhã, Portugal, and with INESC-ID, Inst. Super. Tecn., Univ. Lisbon, Lisbon, Portugal (e-mails: nikpaterak@gmail.com, catalao@ubi.pt).

Ozan Erdinc is with Department of Electrical Engineering, Yildiz Technical University, Istanbul, Turkey (e-mail: oerdinc@yildiz.edu.tr; ozanerdinc@gmail.com).

A. G. Bakirtzis is with the Aristotle University of Thessaloniki (AUTH), Thessaloniki, Greece (e-mail: bakiana@eng.auth.gr).

$T^{h,w,max}$	maximum hot water temperature [°C].
V_{house}	volume of the house [m ³].
ΔT	duration of time interval [h].
δ_{air}	air density [kg/m ³].
λ_t^{buy}	price at which power is bought from the grid [cents/kWh].
λ_t^{sell}	price at which power is sold back to the grid [cents/kWh].
σ_i	element thermal coefficient [J/h·m·°C].
β	roof angle [deg].
C. Variables	
P_t^{AC}	AC power [kW].
$P_t^{ESS,ch}$	ESS charging power [kW].
$P_t^{ESS,dis}$	ESS discharging power [kW].
$P_t^{ESS,sold}$	ESS power injected to grid [kW].
$P_t^{ESS,used}$	ESS power used in household [kW].
$P_t^{EV,ch}$	EV charging power [kW].
$P_t^{EV,dis}$	EV discharging power [kW].
$P_t^{EV,sold}$	EV power injected to grid [kW].
$P_t^{EV,used}$	EV power used in household [kW].
P_t^{EWH}	EWH power [kW].
P_t^{grid}	power drawn from grid [kW].
$P_t^{grid,ex}$	excessive energy drawn from grid [kW].
$P_{m,t}^{mach}$	non-thermostatically controllable appliance power [kW].
$P_t^{PV,sold}$	PV power injected to grid [kW].
$P_t^{PV,used}$	PV power used in household [kW].
P_t^{sold}	power injected back to grid [kW].
S_t^d	deviation of the indoor temperature from the ideal point to down side [°C].
S_t^u	deviation of the indoor temperature from the ideal point to upper side [°C].
SOE_t^{ESS}	ESS state-of-energy [kWh].
SOE_t^{EV}	EV state-of-energy [kWh].
$T_t^{h,w}$	hot water temperature [°C].
T_t^r	room temperature [°C].
u_t^{AC}	binary variable - 1 if AC is operating, else 0.
u_t^{ESS}	binary variable - 1 if ESS is charging, else 0.
u_t^{EV}	binary variable - 1 if EV is charging, else 0.
u_t^{EWH}	binary variable - 1 if EWH is operating, else 0.
u_t^{grid}	binary variable - 1 if power is drawn from the grid, else 0.
$u_{m,p,t}^{ph}$	binary variable - 1 if non-thermostatically controllable appliance is in operating phase p , else 0.
$y_{m,p,t}^{ph}$	binary variable - 1 if non-thermostatically controllable appliance starts operating phase p , else 0.
$z_{m,p,t}^{ph}$	binary variable - 1 if non-thermostatically controllable appliance finishes operating phase p , else 0.

II. INTRODUCTION

A. Motivation and Background

THE smart grid vision aims to enable more active end-user participation rather than just considering them passive consumption points, where smart households have gained increasing interest recently [2]-[3].

Towards enabling smart end-user premises at household level, a home energy management system (HEMS) plays a vital role for the efficient and effective operation of such end-user points coordinated by load serving entities (LSEs) under demand response (DR) strategies [4].

HEMS receives relevant input information (such as pricing data that can be day-ahead, hour-ahead, peak power limits, warnings for planned contingencies, etc.) from LSE and plans the operation of all electrical aspects of the household with a pre-defined aim under imposed constraints by means of LSE restrictions, consumer preferences, among others [5]-[6].

Here, different electrical aspects provide several pros and cons in terms of effective HEMS based operating strategy. There are several types of electrical appliances that can be classified as thermostatically controllable (air conditioners-ACs, electric water heaters-EWHs, etc.), non-thermostatically controllable (washers, dryers, etc.) and non-controllable appliances [7]. Here, as new electrical aspects, electric vehicles (EVs) in terms of a load or even a mobile storage unit, distributed generation (DG) such as roof-top photovoltaic (PV) units, as well as energy storage systems (ESSs) are also gaining importance nowadays within end-user premises with incentives given to local production and use of energy in consumption points in many countries all around the world. To capture the benefits of all such electrical aspects as well as to cover consumer preferences and limitations, an effective HEMS structure is strongly required.

B. Literature Overview

A broad literature is recently dedicated to implementation of different HEMS strategies for smart households.

Chen et al. [11] and Tsui and Chan [12] developed an optimization strategy for the effective operation of a household with a price signal based DR. Li and Hong [13] proposed a “user-expected price” based DR strategy for a smart household, including also a battery based ESS aiming at lowering the total electricity cost by charging and discharging the ESS at off-peak and peak price periods, respectively. However, the impact of including an additional EV load that can also be helpful for peak clipping in certain periods when EV is at home and the possibility of an own production facility have not been evaluated in [13].

Zhao et al. [14] considered the HEMS strategy based control of a smart household, including photovoltaic (PV) based own production facility and availability of EV and ESS. However, vehicle-to-home (V2H) and further possible vehicle-to-grid (V2G) operating modes of EV have not been taken into account in [14]. Restegar et al. [15] developed a smart home load commitment strategy considering all the possible operating modes of EV and ESS. However, that paper neglected the impact of an extra peak power limiting strategy that is probable to be imposed by a LSE, not considered also in [11]-[15].

Pipattanasomporn et al. [16] and Kuzlu et al. [17] presented a HEMS strategy considering peak power limiting DR strategy for a smart household, including both smart appliances and EV charging. Shao et al. [18] also investigated EV for DR based load shaping of a distribution transformer serving a neighborhood.

However, Refs. [16]-[18] did not provide an optimum operating strategy considering price variability with the aim of obtaining the lowest daily cost apart from just limiting peak power drawn from the grid by the household in certain periods.

Matalanas et al. [19] applied an HEMS based on neural networks with experimental results for a household including PV and ESS. However, the impacts of varying price as well as other types of DR strategies have not been evaluated in [19].

Angelis et al. [20] performed the evaluation of a HEMS strategy considering the electrical and thermal constraints imposed by the overall power balance and consumer preferences. Chen et al. [21] provided an appliance scheduling in a smart home considering dynamic prices and appliance usage patterns of a consumer. Missaoui et al. [22] provided a smart building energy management strategy based on price variations and external conditions, as well as comfort requirements. The pricing data based energy management has also been suggested by Hu and Li [23] together with a hardware demonstration. Erdinc [24] considered both pricing and peak power limiting DR, but neglected the possibility of two-way energy trading possibility for EV and ESS with the grid, which can further improve the economic advantage of the HEM structure by increased flexibility. Erdinc et al. [25] imposed distributed renewable energy contribution to reduce load demand on utility side, V2H option of EV to lower the demand peak periods, and two-way energy trading capability of EV (with V2G) and a possible ESS together with different DR strategies. However, the study in [25] neglected the operating strategy of thermal loads such as ACs and EWHs that have a vital role in end-user comfort level supply and energy consumption variation within a residential area. Besides, only a hard peak power limiting strategy and a single type of pricing strategy have been considered in [25] with a time granularity of 1 h that prevents a more detailed analysis of appliance scheduling and impacts of further different DR strategies.

In the literature, there are many methods to formulate a HEMS based optimal in-home power scheduling problem. Methods such as particle swarm optimization [26], genetic algorithms [27], game theory [28], etc. comprise a part in the relevant literature. There are also studies using mixed-integer linear programming (MILP) approach [24, 25]. There are two main advantages of MILP as opposed to other proposed approaches. Firstly, the solution is guaranteed to be global optimum and, secondly, the structure of a MILP model is modular and may be easily modified in order to adapt to required customizations. Finally, there is one more important group of DR studies also including residential consumers that comprise the effect of DR in distribution networks considering power flow and other system operational constraints [29, 30]. However, such considerations are out of the scope of this study.

These papers together with many other studies not referred here have provided valuable contributions to the application of smart grid concepts in household areas. However, many of the mentioned papers failed to address a combined evaluation of V2H operation of EV, impacts of an additional DG, bi-directional operation of ESS, and different appliances including both thermostatically and non-thermostatically types with a sufficiently reduced time granularity under several DR strategies.

C. Contributions

In this paper, a MILP model of the HEM structure is provided to investigate a collaborative evaluation of different pricing and peak power limiting based DR strategies, a PV based DG system, the capability of an EV and ESS based on V2H and ESS-to-home (ESS2H), and different types of both thermostatically and non-thermostatically controllable appliances, AC, EWH, washing machine and dishwasher.

To the best knowledge of the authors, this is the first study in the literature combining all aforementioned operational possibilities in a single HEM system formulated in a MILP framework, which is the main novelty of this paper. Besides, a reduced time granularity (minute-scale) is employed to better analyze the effectiveness of the appliance scheduling part of HEMS strategy. Moreover, a thermal model of the household is also provided to consider the impacts of ambient conditions on in-house thermal dynamics for a more realistic consideration of thermal load operations.

Different case studies including dynamic pricing based, and hard and soft peak power limiting based DR strategies have been conducted. Both economic and technical impacts of these strategies are deeply analyzed in terms of total cost of daily operation and improvement of load factor to have a more flat load pattern that is also the interest of LSE side.

D. Organization

The paper is organized as follows: Section III provides the methodology employed in the study. Afterwards, Section IV includes the case studies for evaluating daily DR based operation strategies for the smart household. Finally, concluding remarks are presented in Section V.

III. MATHEMATICAL FORMULATION

In this section, the formulation of the smart-household energy management system (Fig 1.) under a MILP approach is thoroughly analyzed.

A. Assumptions

In order to mathematically formulate the problem, several assumptions are adopted. Firstly, the degradation of the EV battery by the charging (home to vehicle - H2V) and discharging cycles (V2H and V2G) is neglected considering that the household participates in a battery rental business program offered by EV manufacturers (e.g. Renault [31]). These programs offer a free-of-charge change of EV battery when battery degrades to a level that requires replacement and demands a monthly paid regular rental fee to the manufacturer [32]. Besides, due to fact that the small sized and cheap battery system (such as the mature lead-acid battery technology) considered as ESS in this study has been calculated to have a negligible cost for degradation per cycle compared to electricity rates, the cost that may be related to ESS degradation is also neglected for the sake of simplicity.

The presented model receives the 24-h day-ahead hourly price signal through the smart-meter several hours before its activation. It is to be noted that this is not the actual price that the consumers will pay, but it provides an indication about the expected prices of the next-day. The actual prices are announced in real-time. It is to be stated that this is a common practice in real-life dynamic retail pricing schemes [33].

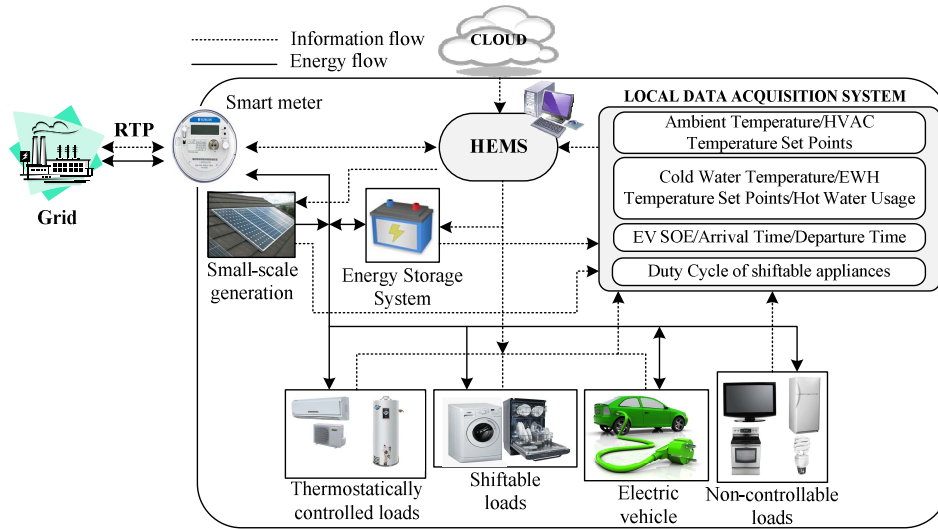


Fig. 1. The smart-household structure.

The presented model receives the 24-h day-ahead hourly price signal through the smart-meter several hours before its activation. It is to be noted that this is not the actual price that the consumers will pay, but it provides an indication about the expected prices of the next-day. The actual prices are announced in real-time. It is to be stated that this is a common practice in real-life dynamic retail pricing schemes [33].

Finally, all the required parameters are considered perfectly known. In practice, an adaptive system that learns from the end-users behavior may be employed or the occupants may insert these data themselves. Parameters such as the ambient temperature may be obtained by forecasts available on-line or by a local data-acquisition system, i.e. a weather station.

The required infrastructure in order to enable the communication between the household elements with the HEMS has been described in [18].

B. Objective Function

The objective is to determine the least cost daily operation of the smart-household by optimally controlling the consumption of several types of appliances. This is expressed by (1).

Minimize

$$Cost = \sum_t (P_t^{grid} \cdot \Delta T \cdot \lambda_t^{buy} - P_t^{sold} \cdot \Delta T \cdot \lambda_t^{sell}) \quad (1)$$

It is to be noted that (1) stands for the actual cost of the household electricity consumption if only a simple day-ahead hourly pricing scheme is active. Other artificial or penalty terms regarding comfort loss or further DR schemes are superimposed to this basic relationship. These are elaborated in the following sections.

Besides, there are also other costs related to the maintenance, replacement etc. of existing components (PV, ESS, etc.) in smart households. However, even if those costs can be assumed also related to the family of “other” operating costs, the manuscript focuses on appliance scheduling based HEMS directly aiming to minimize the reduction of costs associated with the electricity bill of the consumer and, therefore, such additional possible costs are neglected in this study.

C. Constraints

1) Electric Vehicle

The EV model employed in this study is described by (2)-(8). Equation (2) defines the usage of power that comes from discharging the EV (V2H or V2G). Constraints (3) and (4) limit the charging and discharging power of the EV, respectively. The state-of-energy (SOE) of the EV battery is defined by (5) and (6), while (7) stands for the minimum and maximum SOE of the EV in order to avoid deep-discharge. Finally, (8) states that the EV should be fully charged at the end of the time horizon.

$$P_t^{EV,used} + P_t^{EV,sold} = DE^{EV} \cdot P_t^{EV,dis}, \forall t \quad (2)$$

$$0 \leq P_t^{EV,ch} \leq R^{EV,ch} \cdot u_t^{EV}, \forall t \in [T^a, T^d] \quad (3)$$

$$0 \leq P_t^{EV,dis} \leq R^{EV,dis} \cdot (1 - u_t^{EV}), \forall t \in [T^a, T^d] \quad (4)$$

$$SOE_t^{EV} = SOE^{EV,ini} + CE^{EV} \cdot P_t^{EV,ch} \cdot \Delta T - P_t^{EV,dis} \cdot \Delta T \quad (5)$$

$$SOE_t^{EV} = SOE_{t-1}^{EV} + CE^{EV} \cdot P_t^{EV,ch} \cdot \Delta T - P_t^{EV,dis} \cdot \Delta T \quad (6)$$

$$SOE^{EV,min} \leq SOE_t^{EV} \leq SOE^{EV,max}, \forall t \in [T^a, T^d] \quad (7)$$

$$SOE_t^{EV} = SOE^{EV,max}, t = T^d \quad (8)$$

2) Energy Storage System

The constraints that model the operation of the ESS (9)-(14) are similar to the ones describing the operation of the EV. The basic difference is that unlike the EV, the ESS is available at the household premises all day.

$$P_t^{ESS,used} + P_t^{ESS,sold} = DE^{ESS} \cdot P_t^{ESS,dis}, \forall t \quad (9)$$

$$0 \leq P_t^{ESS,ch} \leq R^{ESS,ch} \cdot u_t^{ESS}, \forall t \quad (10)$$

$$0 \leq P_t^{ESS,dis} \leq R^{ESS,dis} \cdot (1 - u_t^{ESS}), \forall t \quad (11)$$

$$SOE_t^{ESS} = SOE_{t-1}^{ESS} + CE^{ESS} \cdot P_t^{ESS,ch} \cdot \Delta T - P_t^{ESS,dis} \cdot \Delta T \quad (12)$$

$$SOE_t^{ESS} = SOE^{ESS,ini}, \text{ if } t = 1 \quad (13)$$

$$SOE^{ESS,min} \leq SOE_t^{ESS} \leq SOE^{ESS,max}, \forall t \quad (14)$$

3) Non-Thermostatically Controllable Loads

A typical household contains loads that operate on a predefined cycle, by means that both the duration of their operation as well as their consumption during operational phases is known (e.g. washing-machine and dishwasher).

The HEMS may shift their operation in order to exploit low-price periods. This type of loads is modelled using (15)-(20). Equation (15) implies that the power that the appliance m is consuming during period t depends on the operating phase that is currently active. Constraint (16) states that a machine cannot be in more than one operating phase simultaneously. Equations (17)-(19) enforce the phase sequence logic. Equation (17) states that the phase p ends exactly $T_{m,p}^{dur}$ periods after it starts. Equation (18) enforces the logic of starting and ending of each phase. Equation (19) states that as soon as a phase finishes, the next phase should immediately start. Finally, (20) enforces the number of times a specific appliance must operate during the horizon. These constraints assume that there is not a user-preference related to when the appliances should perform their task. Nevertheless, if such options need to be considered, desired time limits may be enforced to (15)-(20).

$$P_{m,t}^{mach} = \sum_p u_{m,p,t}^{ph} \cdot P_{m,p}^{ph}, \forall m, t \quad (15)$$

$$\sum_p u_{m,p,t}^{ph} \leq 1, \forall m, t \quad (16)$$

$$y_{m,p,t}^{ph} = z_{m,p,(t+T_{m,p}^{dur})}^{ph} \quad (17)$$

$$y_{m,p,t}^{ph} - z_{m,p,t}^{ph} = u_{m,p,t}^{ph} - u_{m,p,(t-1)}^{ph}, \forall m, p, t > 1 \quad (18)$$

$$z_{m,p,t}^{ph} = y_{m,p+1,t}^{ph}, \forall m, p < card(P), t \quad (19)$$

$$\sum_t y_{m,p,t}^{ph} = N_m, \forall m, p \quad (20)$$

4) Thermostatically Controllable Loads

In this study, the operation of two thermostatically controllable loads, namely the EWH and the AC, is modeled in detail. Such models are important because they are linked with both occupants comfort and high energy consumption, as mentioned before. Especially, the occupants' comfort is a key factor that determines the success of a DR program. However, the operation of such loads depends on the thermal inertia of the water or the air inside the house, which in turn may be exploited in order to address the aforementioned issues.

The EWH model is adapted and suitably modified from [7], being represented by (21)-(24). Specifically, (21) models the water temperature inside the tank considering both the heat exchanges with the environment and the heat provided by the EWH resistance.

It should be stated that the EWH tank is considered to be located in an area that is immediately affected by the ambient air temperature. Furthermore, when hot water is drawn from the EWH, then it is replenished by cold inlet water and the temperature is determined by (22). Lastly, (23) sets the permissible limits of the hot water temperature, while (24) stands for the EWH electric power consumption.

$$T_{t+1}^{h,w} = T_t^a + Q \cdot R \cdot u_t^{EWH} - (T_t^a - T_t^{h,w}) \cdot e^{-\frac{\Delta T}{R \cdot C}}, \quad (21)$$

$$\forall t < T^{max}, m_t = 0$$

$$T_{t+1}^{h,w} = \frac{T_t^{h,w} \cdot (M - m_t) + T_t^{c,w} \cdot m_t}{M}, \forall t < T^{max}, m_t > 0 \quad (22)$$

$$T_t^{h,w,min} \leq T_t^{h,w} \leq T_t^{h,w,max}, \forall t \quad (23)$$

$$P_t^{EWH} = Q \cdot u_t^{EWH}, \forall t \quad (24)$$

An AC may be operated in an interruptible manner in order to reduce its electricity consumption cost. In order to apply this type of operation, a model to determine the temperature inside the house has to be developed. The indoors temperature depends on several factors such as the thermal properties of air, the heat exchange between house and ambient, as well as the thermodynamic properties of the building structure. In this study, a model based on the equivalent thermal resistance of the building is developed. Naturally, this model is based on differential equations that under several plausible assumptions may be linearized [34] as in (25)-(27).

Equation (25) considers only the cooling operation, but it may be easily modified to consider heating as well. The occupants define the required set-point for several periods during which the indoor temperature has to comply (26). The variables S_t^d and S_t^u are positive and define the deviation of the indoor temperature from the ideal point. They may be fixed by the end-user in order to define the AC dead-band (e.g. 1°C around the set-point) or they may be included in the objective function under a high artificial cost in order to minimize the comfort violation. Equation (27) stands for the power used by the AC.

$$T_t^r = \left(1 - \frac{\Delta T}{1000 \cdot M_a c_a R_{eq}}\right) \cdot T_{t-1}^r + \frac{\Delta T}{1000 \cdot M_a c_a R_{eq}} \cdot T_t^a \quad (25)$$

$$- u_{t-1}^{AC} \frac{COP \cdot P_{AC} \cdot \Delta T}{0.000277 \cdot M_a c_a}, \forall t > 1$$

$$SP_t - S_t^d \leq T_t^r \leq SP_t + S_t^u, \forall t: SP_t \neq NaN \quad (26)$$

$$P_t^{AC} = P_{AC} \cdot u_t^{AC}, \forall t \quad (27)$$

Note that thermostatically controllable appliances may be also operated in discrete modes. Such features are consistent with the proposed formulation since the discrete modes of operation of the thermostatically controllable appliances can be modeled by enforcing additional constraints similar to the ones that are enforced for the non-thermostatically controllable appliances.

5) Other Constraints

The power balance is described by (28).

$$P_t^{grid} + P_t^{PV,used} + P_t^{EV,used} + P_t^{ESS,used} = L_t + P_t^{EV,ch} + \sum_m P_{m,t}^{mach} + P_t^{EWH} + P_t^{AC}, \forall t \quad (28)$$

Equation (29) implies that the available PV production may be used to cover household load and if it exceeds it, it is sold back to the grid. Constraints (30), (31) and (32) define the energy transactions between house and grid.

$$P_t^{PV,used} + P_t^{PV,sold} = P_t^{PV,PRO}, \forall t \quad (29)$$

$$P_t^{sold} = P_t^{PV,sold} + P_t^{EV,sold} + P_t^{ESS,sold}, \forall t \quad (30)$$

$$P_t^{grid} \leq PL_1 \cdot u_t^{grid}, \forall t \quad (31)$$

$$P_t^{sold} \leq PL_2 \cdot (1 - u_t^{grid}), \forall t \quad (32)$$

The parameters PL_1 and PL_2 may be used to impose limits to the power that may be drawn or injected back to the grid as a part of an advanced DR strategy. If no power limits are defined, then these parameters are set to sufficiently high positive values.

D. Power Limiting Strategies

The HEMS described by the mathematical model developed previously aims at allocating as much load as possible during lowest price periods.

As a result, a potentially high penetration of smartly operated household loads that operate with a HEMS optimizer raises concerns about causing high power peaks during these periods. This may lead to higher electricity prices during these normally low-demand and low-price periods, distribution transformer overloading, etc. Thus, it is relevant to investigate several power-limiting strategies.

1) "Hard" Power Limit during Several Periods

A power limit may be imposed to the smart-households by responsible entities according to the DR program they participate. The simplest practice is to impose a limit on the power that may be drawn during several periods in order to respond to a contingency or to control the market price. The HEMS is aware of these limits through the smart-meter. To impose such limits, the parameter PL_1 in (31) is substituted by a time-varying limit PL_1^t . Nevertheless, this strategy may still lead to several other peaks due to load recovery effect.

2) "Soft" Power Limit during the Day

The "hard" limit may be imposed only for several hours while a DR event is in progress. Another strategy that may be used in order to control the maximum power drawn by the grid throughout the day is described by (33). Firstly, a power limit PL_1^t is set for the applicable periods. The household is allowed to draw power that exceeds this limit, but the excessive energy is penalized. In this study, it is considered that the excessive energy is priced with the highest hourly price augmented by a percentage a (e.g. 10%). This strategy is a combination of time-varying DR and critical peak pricing [35].

$$P_t^{grid} \leq PL_1^t + P_t^{grid,ex}, \forall t \quad (33)$$

Under this scheme, the objective function is transformed to (34).

$$Cost = \sum_t \left\{ \begin{array}{l} (P_t^{grid} - P_t^{grid,ex}) \cdot \Delta T \cdot \lambda_t^{buy} \\ + P_t^{grid,ex} \cdot \Delta T \cdot (1 + a) \cdot \max_t(\lambda_t^{buy}) \\ - P_t^{sold} \cdot \Delta T \cdot \lambda_t^{sell} \end{array} \right\} \quad (34)$$

3) Assessment of Power Limiting Strategy

Generally, it may be desirable to obtain a power consumption curve as flat as possible in order to achieve better controllability of a load at a certain part of the DS. The end-users may be given incentives in order to achieve a certain value of the load factor (LF) index described by (35), which stands for the ratio of the average net power drawn from the grid to the peak power. The higher the value of this index, the more flat the power curve of the household is.

$$LF = \frac{avg_t(P_t^{grid} - P_t^{sold})}{\max_t(P_t^{grid} - P_t^{sold})} \quad (35)$$

Another fact that is important in order to assess the potential macroscopic impacts of the proposed strategies on the operation of the power system is the load fluctuations that are caused by the operation of the HEMS. Steep increase or decrease in the load may require more regulation capacity to be employed by the System Operator (SO), especially as the penetration of smart-grid enabling technologies is increasing in the residential sector. For this reason, the average ramping index (ARI) that is a modified variant of the load turbulence index [36] is introduced (36).

$$ARI = \frac{1}{card(T)} \sum_t |(P_t^{grid} - P_t^{sold}) - (P_{t-1}^{grid} - P_{t-1}^{sold})| \quad (36)$$

To facilitate the regulation of the load it is desirable to have low MLTI values. Considering that more customers would enroll to such programs in the future, more severe power peaks could occur during relatively low price periods, causing violations to the voltage and current limits of the distribution system and increase market price volatility [30]. As a result, a criterion according to which a DR strategy should be evaluated is the smoothness of the induced load profile.

IV. TESTS AND RESULTS

A. Input Data

Firstly, the selected time-window for the optimization is 5 min (0.0833h). The household comprises several loads, the rated power of which can be found in Table I. The inflexible load consumption over the scheduling horizon is presented in Fig. 2 for a 4-member household together with the installed PV system's (1kW) available production. The load profile in Fig. 2 is gathered from the real appliances based load profile generation [37]. Besides, PV production is a real measurement from a 1 kW roof-top PV system.

Apart from these loads, a Chevy Volt (EV) is also considered. It is employed with a charging station that has a charging power limited to 3.3kW while its battery rating is 16kWh [10]. The charging efficiency is considered 95%. It should be noted that the EV arrives at home at 5pm and needs to be fully charged at 6:55am of the next day. Its initial SOE is considered 8kWh (50%). To avoid deep discharge, the lowest limit is set to 4.8kWh (30%).

The washing-machine and the dishwasher are considered controllable loads. Their operating cycle is described in Table II [38]. The washing machine consumes 2 kW during the heating phase, 0.15 kW during the washing and rinsing phase, and 0.3 kW during the spinning phase. The dishwasher consumes 2.2 kW for the washing, hot rinsing and drying phases, and 0.15 kW for the cold rinse phase.

For the EWH the water usage pattern and the set points are required. It is assumed that the shower head has a flow of 2.5 gallons/min, while each shower lasts 10 minutes (2 periods). During the shower the water temperature should not be less than 40°C. The occupants are assumed to take showers at 7:50am, 1:30pm and 8:30pm. During the horizon, the water temperature inside the EWH tank may not exceed 60°C for safety reasons. The EWH is considered to be located in an area where the temperature is not affected by AC operation. Its rated power is 2kW and its water capacity is 50 gallons. Other thermal properties of the EWH are the same as in [7].

To control the consumption of the AC, the equivalent thermal resistance of the house as well as the mass of air inside it are both required. These calculations may be performed using equations (37)-(39) considering a rectangular geometry and an inclination of the roof of β° [20]

$$R^{eq} = \frac{1}{N} \sum_i \frac{l_i}{\sigma_i A_i} \quad (37)$$

$$V_{house} = L_1 \cdot L_2 \cdot L_3 + \tan(\beta) \cdot L_1 \cdot L_2 \quad (38)$$

$$M_a = V_{house} \cdot \delta_{air} \quad (39)$$

TABLE I. HOUSEHOLD APPLIANCES DATA

Appliance	Rated Power (kW)	Periods (5-min)	Appliance	Rated Power (kW)	Periods (5-min)
Refrigerator	1.67	288	Desktop Computer	0.15	24
Iron	2.4	6	Hair Straightener	0.055	2
Toaster	0.8	2	Oven	2.4	13
Kettle	2	2	Cooker hood	0.225	13
Hairdryer	1.8	3	Lighting	0.1	90
Telephone	0.005	288	Other (fixed)	0.1	288
TV	0.083	158			

TABLE II. OPERATING PHASES OF THE APPLIANCES

Appliance	phase	1	2	3	4	5	6	7
		Power (kW)	0.15	2	0.15	2	0.15	0.3
Washing Machine	Duration (periods)	1	3	3	1	3	6	1
	Power (kW)	2.2	0.15	2.2	-	-	-	-
Dishwasher	Duration (periods)	7	8	6	-	-	-	-

TABLE III. STRUCTURAL PARAMETERS OF THE SMART-HOUSEHOLD

Parameter	Value	Units	Parameter	Value	Units
House Length (L_1)	30	m	Area of Windows	1	m ²
House Width (L_2)	10	m	Wall thermal coefficient	136.8	J/h·m·°C
House Height (L_3)	4	m	Window thermal coefficient	2808	J/h·m·°C
Roof Angle (β)	40	deg	Thickness of windows	0.05	m
Number of Windows	6	-	Thickness of walls	0.15	m

Generally, the density of the air and its thermal capacity depend on its thermodynamic properties (temperature, pressure, etc.). In this study, they are considered constant and utilize standard values $\delta_{air} = 1.225 \text{ kg/m}^3$ and $c_a = 1.01 \text{ kJ/kg}^\circ\text{C}$. Data concerning the structural parameters of the house are presented in Table III. For the given data the equivalent thermal resistance is $3.1965 \cdot 10^{-6} \frac{\text{h}\cdot^\circ\text{C}}{\text{J}}$. The volume of the house is 1451.729 m^3 and as a result the mass of air is 1778.369 kg . Furthermore, the AC unit has a rated power of 2 kW and the coefficient-of-performance (COP) is 2. The occupants set the thermostat set-point to 25°C from 12:30pm to 9pm. The dead-band of the thermostat is set to 0.5°C around the set point.

The outdoors temperature for a hot summer day and the inlet water temperature are given in Fig. 3. The temperature is adapted from hourly measured values in Heraklion, Crete, Greece during July 2014. Detailed data for the inlet water temperature are scarce and as a result for the purposes of our study are constructed as follows: firstly, an average temperature is considered (20°C). Then, due to the high thermal capacity of the ground, it is considered that air temperature affects the inlet water temperature very little (e.g. a positively superimposed factor of $1/7$). Lastly, Gaussian noise is added at the temperature in the range of -0.5°C to 0.5°C . The smart-meter receives the 24-h price signal presented in Fig. 4 that corresponds to a typical summer day. Day-ahead hourly prices are adapted from [33]. The PV power may be injected back at a feed-in tariff (FIT).

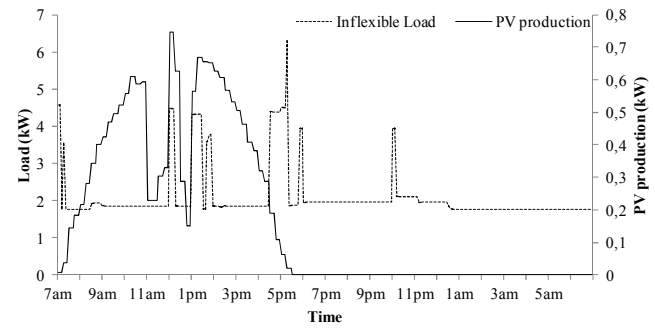


Fig. 2. Inflexible load demand and PV production.

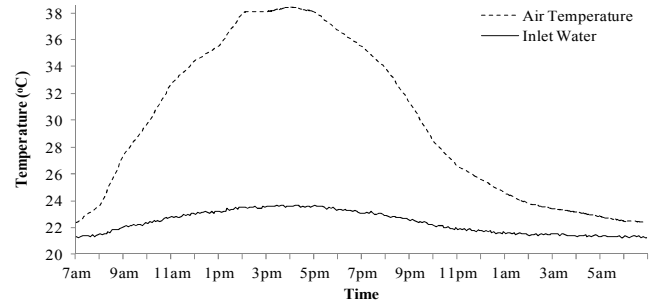


Fig. 3. Outside air temperature and inlet water temperature.

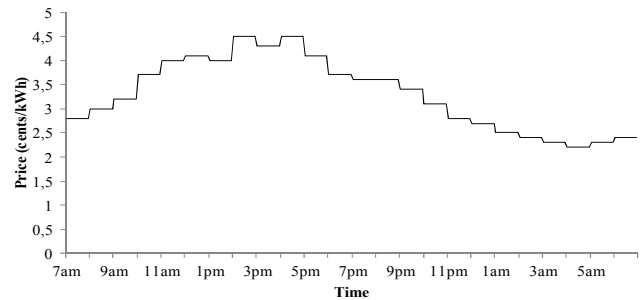


Fig. 4. Day-ahead hourly pricing signal.

B. Simulation Results and Discussion

The presented simulations aim mainly at assessing the capability of the EMS to respond not only to the dynamic pricing in order to allocate the household load in the least-cost operation, but also to specific load-shape requirements imposed by the grid operator. In this respect, the capability of the household to sell energy back to the grid complicates the analysis. Besides, the pricing policy of selling energy back to the grid (dynamic selling-back price, FIT, etc.) may affect the result and thus a separate analysis is required. Nevertheless, this is out of the scope of this study. In this respect, in this study it is considered that the household may not sell back energy to the grid.

Figs. 5-7 depict the power drawn from the grid during the day, while Figs. 8-10 illustrate the hourly energy allocation to the different loads as well as the energy contribution of EV, ESS, PV and grid. In case no power restriction is set to the smart-household (Figs. 5 and 8), the HEMS allocates the loads to the least-price periods causing peaks to emerge early in the morning. Then, a “hard” limit is considered to be active from 12am to 6:55am, periods in which the electricity prices are the lowest within the day and therefore a high load is expected to occur.

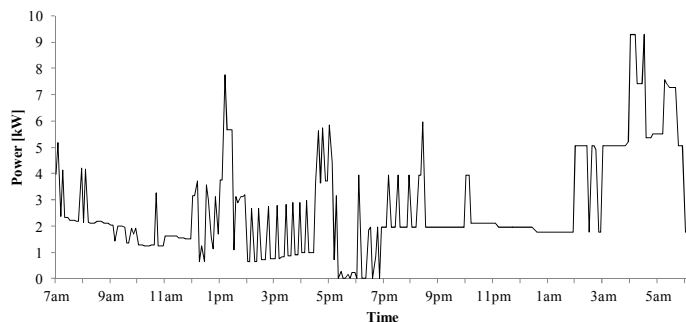


Fig. 5. Power drawn from the grid (no power limit).

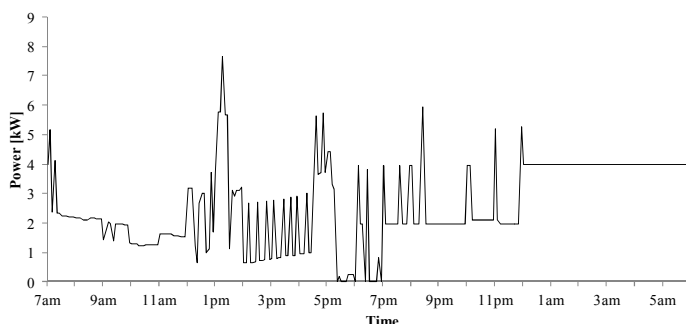


Fig. 6. Power drawn from the grid (4kW- 12am-6:55am).

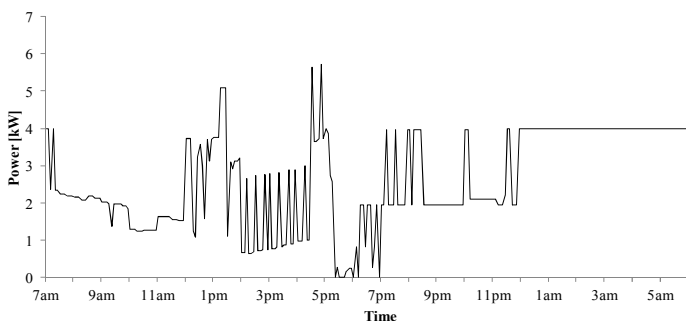


Fig. 7. Power drawn from the grid (4kW- "soft" limit).

As can be noticed in Figs. 6 and 9, during these periods the load is reduced to 4kW and as a result the EV is forced to charge using less power for a longer period. Similarly, the dishwasher and the washing machine are shifted. Before 11pm the load remains essentially the same as the one of the previously described case.

Figs. 7 and 10 correspond to the case where a power limit equal to 4kW is enforced throughout the time horizon, allowing for violations under a penalty that is equal to 10% of the highest price of the day. As it can be noticed in Fig. 10, for the periods after 11pm the results are similar to the ones of the "hard" limit case. The ESS provides energy to the home during 7am and 1pm in order to eliminate the peak caused mainly by the non-controllable loads operating during this hour. Furthermore, the EWH and the AC are operated for a longer time in order to store energy by means of hot water and building structure thermal inertia, respectively.

To sum up, comparing Figs. 5-7 demonstrates that the effect of limiting the power that may be drawn from the grid through a power-limiting DR strategy in combination with the price-based DR, is the re-distribution of the load among the lowest-price periods that coincide with the hard power limit (Fig. 6).

In case of the "soft" power limit, excessive power can be procured, but HEMS prevents this in order to avoid being penalized. Besides, comparing Figs. 8-10 the re-scheduling of different appliances can be better observed by the shifting of the loads such as EV charging, washing machine, dishwasher etc., as mentioned before. To better illustrate the effects of power limiting strategies, a parametric analysis is performed and the results concerning the cost and the LF are presented in Table IV. The "hard" power limiting strategy guarantees that peaks do not occur during 12am-6:55am. This leads to an improved load factor for all cases. Cost increases by imposing a stricter power limit because of shifting energy consumption to relatively higher price periods for hourly pricing scheme.

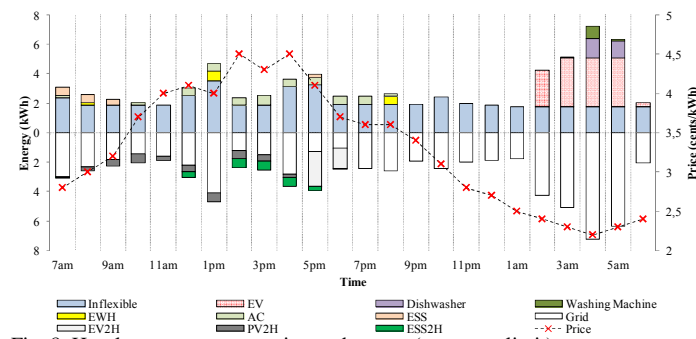


Fig. 8. Hourly energy consumption and source (no power limit).

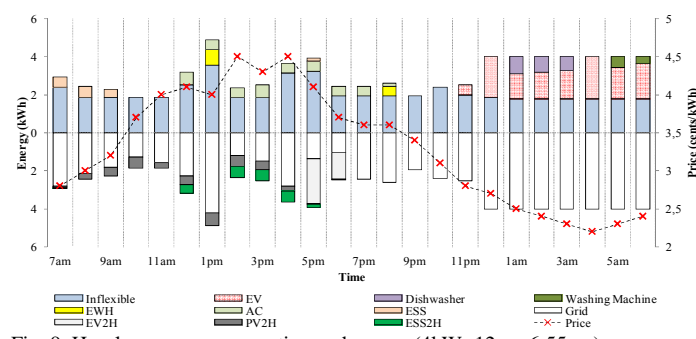


Fig. 9. Hourly energy consumption and source (4kW- 12am-6:55am).

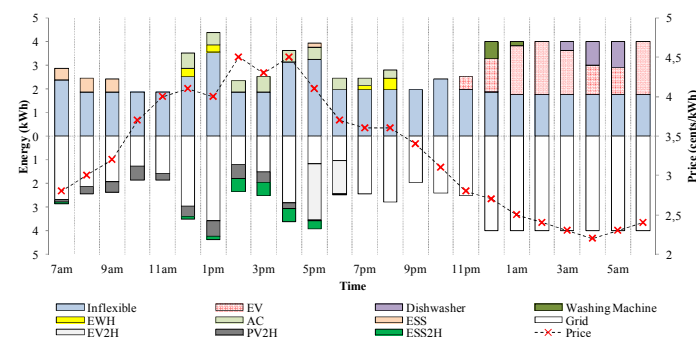


Fig. 10. Hourly energy consumption and source (4kW - "soft" limit).

TABLE IV. COMPARISON OF DR STRATEGIES COST AND LOAD FACTOR UNDER HOURLY PRICING

Case		Cost (€)	LF
No Power Limit	-	1.953	0.288
"Hard" Power Limit from 12am to 6:55am	6kW	1.956	0.348
	5kW	1.958	0.349
	4kW	1.979	0.349
"Soft" Power Limit	6kW	1.954	0.444
	5kW	1.960	0.467
	4kW	1.976	0.466
	3kW	2.064	0.465

TABLE V. COMPARISON OF OPTIMAL COSTS FOR DIFFERENT EV PARAMETERS

Case	Initial SOE (kWh)	EV arrival time	Cost (€)
Base case	8	5:05 pm	1.953
C1	8	2:15 pm	1.941
C2	8	9:30 pm	1.989
C3	6.3	5:05 pm	2.021
C4	6.3	2:15 pm	2.013
C5	6.3	9:30 pm	2.041
C6	13.5	5:05 pm	1.769
C7	13.5	2:15 pm	1.727
C8	13.5	9:30 pm	1.851

TABLE VI. LOAD SHAPING EFFECT OF ESS CAPACITY

Case	ESS Capacity (kWh)	No Power Limit			Soft power limit of 5 kW		
		LF	ARI (kW)	Cost (€)	LF	ARI (kW)	Cost (€)
C1	0	0.290	0.523	2.005	0.427	0.398	2.024
C2	1	0.289	0.565	1.989	0.439	0.438	2.005
C3	2	0.289	0.662	1.977	0.452	0.459	1.986
Base case	3	0.288	0.674	1.953	0.466	0.467	1.960
C4	4	0.287	0.677	1.945	0.469	0.491	1.955
C5	5	0.285	0.668	1.926	0.496	0.507	1.933
C6	6	0.285	0.704	1.913	0.512	0.468	1.916

The “soft” power limiting strategy results into flattening the load curve in comparison with the case in which no power limit is imposed. An increase in the cost of the power drawn from the grid is noticed because of two factors: controllable load is shifted to periods with greater price and also the excessive energy, mainly because of inflexible load, is penalized. It is also noticed that as the “soft” power limit becomes lower, the load factor is no longer improved; instead, it slightly decreases. This is caused by the fact that the energy that may be provided by the household assets (EV, ESS and PV) to reduce power drawn from the grid to cover inflexible load is limited, and thus it is not possible to mitigate peaks.

In order to evaluate how different consumer behaviors affect the optimal operational cost of the smart households, different cases of initial EV SOE and EV arrival time are investigated and the relevant results are presented in Table V. It can be noticed that as the EVs arrive later in the day, the operational cost increases since they offer energy to cover a portion of the household load via V2H during less costly periods that in turn is covered by energy purchased by the grid during higher price periods. Another observation is that the increase of the initial SOE by 40.7% renders a 10.8% decrease in the operational cost, whilst the reduction of 21.2% in the initial SOE results in 2.9% higher daily energy procurement cost, considering that the EV arrival time is 5:05 pm.

To complete the analysis of the proposed HEMS model, the impact of ESS as a load shaping mechanism is studied (Table VI) both for unconstrained operation of the smart household and considering a “soft” power limit DR strategy of 5 kW throughout the day. The ESS capacity varies between 0 and 6 kWh. Note that the initial SOE of the ESS is considered 50% of the capacity and the charging/discharging rates are adjusted so that 20% of this capacity can be charged/discharged per hour. Lastly, the minimum allowable ESS capacity is considered 25% of the maximum capacity. First of all, it may be noticed that in the case in which no power limitation is imposed, increasing the ESS capacity results into a decrease in the LF and an increase in the ARI indices, respectively. From the perspective of the SO, the increased flexibility

offered by the higher capacity of the ESS to the end-user results into a fluctuating load profile that can macroscopically pose challenges for the system operation (i.e. load balancing) as the penetration of smart technologies increases in the residential sector. When the “soft” limit DR strategy is enforced, the ESS appears to have a different role. As the capacity of ESS increases, it can be noticed that LF also increases, as a result of the HEMS being forced to reduce the peaks to avoid being penalized. Furthermore, the ARI is also reduced compared to the previous case of not enforcing the DR strategy. Note that, in all cases, increasing the capacity of the ESS results into reduced costs.

C. Practical Applicability of the Proposed Approach

The 5-minute time frame is adequate in order to describe in detail the use of several household appliances, such as a hairdryer as well as user behavior (arrival time of EV, duration of showers, etc.). In general, the number of constraints and variables is indicative of the computational burden associated with the developed model, which in turn highly depends on the adopted time granularity.

The model has been coded in GAMS 24.0.2 and has been solved by the commercial solver CPLEX 12. The dimensions of the computationally worst simulation are noticeable: 18769 constraints, 20084 variables and 13413 binary variables. The average solution time, considering an optimality gap of 0%, is 16 sec on a modern laptop computer (i7 at 2.4GHz, 4GB of RAM, 64bit Windows) and less than 1 sec in a workstation (two 6-core processors at 3.46 GHz, 96 GB of RAM, 64-bit Windows).

As the computational capabilities of embedded systems that are needed to implement HEMS and monitoring systems increase, it appears that such complex algorithms will be practically applicable even for larger scale systems. As a result, the model presented in this study may indeed be effectively employed in real-life real-time applications.

V. CONCLUSIONS

In this study, a HEMS structure has been described where thermostatically and non-thermostatically controllable loads were explicitly modeled using MILP. ESS and DG were also considered. The aim of the optimization problem was to minimize the total cost to meet the electrical energy needs of the household in a dynamic pricing environment. Furthermore, the effect of several load-shaping strategies based on hard and soft peak power limiting DR was investigated. Then, the model was tested using a realistic test case with sufficiently low level of time granularity and the results were thoroughly discussed. Based on the simulations conducted, despite the considerable complexity of the mathematical model, the model proved to be computationally efficient.

VI. REFERENCES

- [1] R. A. S. Fernandes, I. N. da Silva, and M. Oleskovicz, “Load Profile Identification Interface for Consumer Online Monitoring Purposes in Smart Grids,” *IEEE Trans. Industrial Informatics*, vol. 9, pp. 1507-1607, Aug. 2013.
- [2] K. H. S. V. S. Nunna, and S. Doolla, “Responsive End-User-Based Demand Side Management in Multimicrogrid Environment,” *IEEE Trans. Industrial Informatics*, vol. 10, pp. 1262-1272, May 2014.
- [3] O. Kilkki, A. Alahaivala, and I. Seilonen, “Optimized Control of Price-Based Demand Response with Electric Storage Space Heating,” *IEEE Trans. Industrial Informatics*, vol. 11, pp. 281-288, Feb. 2015.
- [4] A. Safdarian, M. F. Firuzabad, and M. Lehtonen, “A Distributed Algorithm for Managing Demand Response in Smart Grids,” *IEEE Trans. Industrial Informatics*, vol. 10, pp. 2385-2393, Nov. 2014.
- [5] K. Basu, V. Debusschere, S. Bacha, U. Maulik, and S. Bondyopadhyay, “Non Intrusive Load Monitoring: A Temporal Multi-Label Classification Approach,” *IEEE Trans. Industrial Informatics*, vol. 11, pp. 262-270, Feb. 2015.

[6] G. Graditi, M. L. Di Silvestre, R. Gallea, and E. R. Sanseverino, "Heuristic-Based Shiftable Loads Optimal Management in Smart Micro-Grids," *IEEE Trans. Industrial Informatics*, vol. 11, pp. 271-280, Feb. 2015.

[7] P. Du, and N. Lu, "Appliance Commitment for Household Load Scheduling," *IEEE Trans. Smart Grid*, vol. 2, pp. 411-419, June 2011.

[8] J. C. Ferreira, V. Monteiro, and J. L. Afonso, "Vehicle-to-Anything Application (V2Anything App) for Electric Vehicles," *IEEE Trans. Industrial Informatics*, vol. 10, pp. 1927-1937, Aug. 2014.

[9] C. Chen, and S. Duan, "Optimal Integration of Plug-In Hybrid Electric Vehicles in Microgrids," *IEEE Trans. Industrial Informatics*, vol. 10, pp. 1917-1926, Aug. 2014.

[10] GM Chevy Volt Specifications [Online]. Available: <http://gm-volt.com/full-specifications/>

[11] Z. Chen, L. Wu, and Y. Fu, "Real-time price-based demand response management for residential appliances via stochastic optimization and robust optimization," *IEEE Trans. Smart Grid*, vol. 3, pp. 1822-1831, Dec. 2012.

[12] K. M. Tsui, and S. C. Chan, "Demand response optimization for smart home scheduling under real-time pricing," *IEEE Trans. Smart Grid*, vol. 3, pp. 1812-1821, Dec. 2012.

[13] X. Li, and S. Hong, "User-expected price-based demand response algorithm for a home-to-grid system," *Energy*, vol. 64, pp. 437-449, Jan. 2014.

[14] J. Zhao, S. Kucuksari, E. Mazhari, and Y. J. Son, "Integrated analysis of high-penetration PV and PHEV with energy storage and demand response," *Applied Energy*, vol. 112, pp. 35-51, Dec. 2013.

[15] M. Rostegar, M. F. Firuzabad, and F. Aminifar, "Load commitment in a smart home," *Applied Energy*, vol. 96, pp. 45-54, Aug. 2012.

[16] M. Pipattanasomporn, M. Kuzlu, and S. Rahman, "An Algorithm for Intelligent Home Energy Management and Demand Response Analysis," *IEEE Trans. Smart Grid*, vol. 3, pp. 2166-2173, Dec. 2012.

[17] M. Kuzlu, M. Pipattanasomporn, and S. Rahman, "Hardware demonstration of a home energy management system for demand response applications," *IEEE Trans. Smart Grid*, vol. 3, pp. 1704-1711, Dec. 2012.

[18] S. Shao, M. Pipattanasomporn, and S. Rahman, "Demand response as a load shaping tool in an intelligent grid with electric vehicles," *IEEE Trans. Smart Grid*, vol. 2, pp. 624-631, Dec. 2011.

[19] E. Matallanas, M. C. Cagigal, A. Gutierrez, F. M. Huelin, E. C. Martin, D. Masa, and J. J. Leube, "Neural network controller for active demand-side management with PV energy in the residential sector," *Applied Energy*, vol. 91, pp. 90-97, Mar. 2012.

[20] F. de Angelis, M. Boaro, S. Squartini, F. Piazza, and Q. Wei, "Optimal Home Energy Management under Dynamic Electrical and Thermal Constraints," *IEEE Trans. Industrial Informatics*, vol. 9, pp. 1518-1527, Aug. 2013.

[21] X. Chen, T. Wei, and S. Hu, "Uncertainty-aware household appliance scheduling considering dynamic electricity pricing in smart home," *IEEE Trans. Smart Grid*, vol. 4, pp. 932-941, June 2013.

[22] R. Missaoui, H. Joumaa, S. Ploix, and S. Bacha, "Managing energy smart homes according to energy prices: Analysis of a building energy management system," *Energy and Buildings*, vol. 71, pp. 155-167, Mar. 2014.

[23] Q. Hu, and F. Li, "Hardware design of smart home energy management system with dynamic price response," *IEEE Trans. on Smart Grid*, vol. 4, pp. 1878-1887, Dec. 2013.

[24] O. Erdinc, "Economic impacts of small-scale own generating and storage units, and electric vehicles under different demand response strategies for smart households," *Applied Energy*, vol. 126, pp. 142-150, Aug. 2014.

[25] O. Erdinc, N.G. Paterakis, T.D.P. Mendes, A.G. Bakirtzis, and J.P.S. Catalao, "Smart Household Operation Considering Bi-Directional EV and ESS Utilization by Real-Time Pricing-Based DR," *IEEE Trans. Smart Grid*, in press, doi: 10.1109/TSG.2014.2352650.

[26] M.A.A. Pedrasa, T. D. Spooner, and I. F. MacGill, "Coordinated scheduling of residential distributed energy resources to optimize smart home energy services," *IEEE Trans. Smart Grid*, vol. 1, pp. 134-143, Sep. 2010.

[27] Z. Zhao, W. C. Lee, Y. Shin, and K. B. Song, "An Optimal Power Scheduling Method for Demand Response in Home Energy Management System," *IEEE Trans. Smart Grid*, vol. 4, pp. 1391-1400, Sep. 2013.

[28] A.-H. Mohesnian-Rad, V. W. S. Wong, J. Jatskevich, R. Schober, and A. Leon-Garcia, "Autonomous demand-side management based on game theoretic energy consumption scheduling for the future smart grid," *IEEE Trans. Smart Grid*, vol. 1, no. 3, pp. 320-331, Dec. 2010.

[29] A.-H. Mohesnian-Rad, and A. Davoudi, "Towards Building an Optimal Demand Response Framework for DC Distribution Networks," *IEEE Trans. Smart Grid*, vol. 5, pp. 2626-2634, Sept. 2014.

[30] W. Shi, N. Li, X. Xie, C.C. Chu, and R. Gadh, "Optimal Residential Demand Response in Distribution Networks," *IEEE Journal on Selected Areas in Communications*, vol. 32, pp. 1441,1450, July 2014.

[31] Leasing a battery for an electric car [online]. Available: <http://www.which.co.uk/cars/choosing-a-car/buying-a-car/buying-vs-leasing/leasing-a-battery-for-an-electric-car/>

[32] Your Questions, Answered: Is The Renault Fluence a Good Used Car Buy? [online]. Available: <http://transportevolved.com/2013/11/25/your-questions-answered-is-the-renault-fluence-a-good-used-car-buy/>

[33] ComEd residential real-time pricing program [online]. Available: <http://rrtp.comed.com>

[34] H. Wang, K. Meng, F. Luo, Z. Y. Dong, G. Verbic, Z. Xu, and K.P. Wong, "Demand Response Through Smart Home Energy Management Using Thermal Inertia," in *Proc. 2013 Australasian Universities Power Engineering Conference*, pp. 1-6.

[35] Demand Response Directory [Online]. Available: <http://www.demandresponsedirectory.com>

[36] E. Heydarian-Forushani, M.P. Moghaddam, M.K. Sheikh-El-Eslami, M. Shafiekhah, and J.P.S. Catalão, "A stochastic framework for the grid integration of wind power using flexible load approach," *Energy Conversion and Management*, vol. 88, pp. 985-998, Dec. 2014.

[37] A. Tascikaraoglu, A.R. Boynuegri, and M. Uzunoglu, "A Demand Side Management Strategy Based on Forecasting of Residential Renewable Sources: A Smart Home System in Turkey," *Energy and Buildings*, vol. 80, pp. 309-320, Sept. 2014.

[38] R. Missaoui, H. Joumaa, S. Ploix, and S. Bacha, "Managing Energy Smart Homes According to Energy Prices: Analysis of a Building Energy Management System," *Energy and Buildings*, vol. 71, pp. 155-167, 2014.

BIOGRAPHIES



Nikolaos G. Paterakis (S'14) received the Dipl. Eng. Degree from the Department of Electrical and Computer Engineering, Aristotle University of Thessaloniki, Thessaloniki, Greece, in 2013. Since September 2013 he has been with University of Beira Interior, Covilhã, Portugal, working towards the Ph.D. degree under EU FP7 Project SiNGULAR.

His research interests are in power system operation and planning, renewable energy integration, ancillary services, demand response and smart grid applications.



Ozan Erdinc (M'14) received the B.Sc., M.Sc. and Ph.D. degrees from Yildiz Technical University, Istanbul, Turkey, respectively in 2007, 2009, 2012. He has been a Post-Doctoral Fellow under EU FP7 project "SiNGULAR" at University of Beira Interior (UBI), Covilhã, Portugal since May 2013. Besides, from February 2014 to January 2015, he worked as an assistant professor at the Electrical-Electronics Engineering Department of Istanbul Arel University, Istanbul, Turkey. On January 2015, he joined the Electrical Engineering Department of Yildiz

Technical University, Istanbul, Turkey as an assistant professor where he is still working. His research interests are hybrid renewable energy systems, electric vehicles, power system operation and smart grid technologies.



Anastasios G. Bakirtzis (S'77-M'79-SM'95-F'15) received the Dipl. Eng. Degree from the Department of Electrical Engineering, National Technical University, Athens, Greece, in 1979 and the M.S.E.E. and Ph.D. degrees from Georgia Institute of Technology, Atlanta, in 1981 and 1984, respectively. Since 1986 he has been with the Electrical Engineering Department, Aristotle University of Thessaloniki, Greece, where he is currently Professor. His research interests are in power system operation, planning and economics.



João P. S. Catalão (M'04-SM'12) received the M.Sc. degree from the Instituto Superior Técnico (IST), Lisbon, Portugal, in 2003, and the Ph.D. degree and Habilitation for Full Professor ("Agregação") from the University of Beira Interior (UBI), Covilhã, Portugal, in 2007 and 2013, respectively.

Currently, he is a Professor at UBI, Director of the Sustainable Energy Systems Lab and Researcher at INESC-ID. He is the Primary Coordinator of the EU-funded FP7 project SiNGULAR ("Smart and Sustainable Insular Electricity Grids Under Large-Scale Renewable Integration"), a 5.2 million euro project involving 11 industry partners. He has authored or coauthored more than 350 publications, including 110 journal papers, 220 conference proceedings papers and 20 book chapters, with an *h*-index of 24 (according to Google Scholar), having supervised more than 25 post-docs, Ph.D. and M.Sc. students. He is the Editor of the book entitled *Electric Power Systems: Advanced Forecasting Techniques and Optimal Generation Scheduling* (Boca Raton, FL, USA: CRC Press, 2012), translated into Chinese in January 2014. Currently, he is editing another book entitled *Smart and Sustainable Power Systems: Operations, Planning and Economics of Insular Electricity Grids* (Boca Raton, FL, USA: CRC Press, 2015). His research interests include power system operations and planning, hydro and thermal scheduling, wind and price forecasting, distributed renewable generation, demand response and smart grids.

Prof. Catalão is an Editor of the IEEE TRANSACTIONS ON SMART GRID, an Editor of the IEEE TRANSACTIONS ON SUSTAINABLE ENERGY, and an Associate Editor of the *IET Renewable Power Generation*. He was the Guest Editor-in-Chief for the Special Section on "Real-Time Demand Response" of the IEEE TRANSACTIONS ON SMART GRID, published in December 2012, and he is currently Guest Editor-in-Chief for the Special Section on "Reserve and Flexibility for Handling Variability and Uncertainty of Renewable Generation" of the IEEE TRANSACTIONS ON SUSTAINABLE ENERGY. He is the recipient of the 2011 Scientific Merit Award UBI-FE/Santander Universities and the 2012 Scientific Award UTL/Santander Totta.